A New Advance in Circular Polarization Selective Surface—A Three Layered CPSS Without Vertical Conductive Segments

I-Young Tarn and Shyh-Jong Chung, *Senior Member, IEEE*

***Abstract*—Investigations into a surface that reflects one sense of circularly polarized electromagnetic wave but transmits the other, namely a circular-polarization selective surface (CPSS), were carried out. This paper presents CPSS using simple planar structure without any vertical conductive segments. Couplings, through the use of L-shaped traces, were produced to replace the vias. Operational principle and design procedure are developed, thus the optimal design parameters are found. Also presented are the results of numerical computations and measurements for "isolation" and "transmission loss". A 30 GHz example demonstrates the performances of the design and the attractiveness in millimeter-wave circular polarization selectivity applications.**

***Index Terms*—Circular-polarization selective surface (CPSS), coupling, isolation, printed circuit board (PCB), transmission loss.**

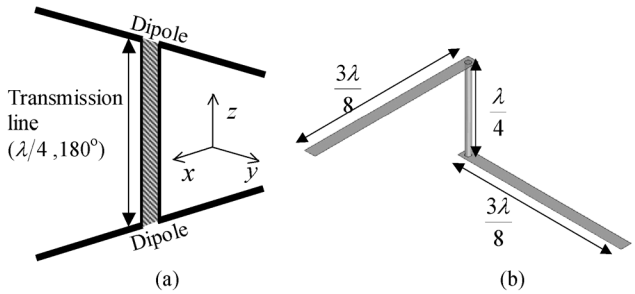

Fig. 1. (a) The constituent element of the CPSS structure proposed in [6]. (b) The constituent element of the CPSS structure proposed in [7].

I. Introduction

LINEAR-polarization selective surfaces in modern reflector antenna design, such as reflectarray antennas [1]–[4], have been known and used for a long time. Many applications, stemmed from linear polarization (LP) selection could be converted to applications based on circular polarization (CP) selection, e.g., satellite communications, navigation systems, wireless LAN, automotive radar, and remote sensing radar applications. On the other hand, CPSS has been rarely used since no simple electromagnetic surface achieving such a selection is accredited yet.

A lossless and perfect CPSS would pass one sense of CP wave while reflecting the other. Based on the reciprocity theorem, it is easy to derive that the reflected wave for the reflection case, possesses the same polarization sense as the incident wave, and the transmitted wave for the transmission case must be of the same polarization as the incoming wave. Therefore, an ideal left-hand circular-polarization selective surface (LHCPSS) would thoroughly reflect a left-hand circularly polarized (LHCP) incident wave, while at the same time be completely transparent to a right-hand circularly polarized (RHCP) incident wave. Likewise, an ideal right-hand circular-polarization selective surface (RHCPSS) would be opaque to a right-hand circularly polarized (RHCP) wave and yet transparent to a LHCP wave.

Conventional circular polarization selective structures comprise transverse metal traces on different layers jointed together with longitudinal conductive filaments. Two typical designs are shown in Fig. 1. Besides, assemble two or more CP polarizers or LP-CP converters [5] with specified separations and orientations could achieve the same circular polarization selectivity function.

The initial concept was introduced in [6], which proposed a CPSS formed by a two-dimensional array. Each array element consisted of two orthogonal and resonant dipoles, separated by a free-space quarter wavelength in height; with their center feed points connected together by a half-wavelength transmission line, as shown in Fig. 1(a).

The above design is intuitive, but there exist problems in practice. The main difficulty is that the geometry and the medium of the transmission line must be properly designed to make the separation of the two dipoles a quarter wavelength and the electrical length a half wavelength simultaneously. In addition, considerations must be taken to maintain impedance matching between the dipoles and the transmission line. Thus realizing this structure for use in high frequencies is not easy. As a result of the complexity, another design with an analogous concept but simpler structure was discovered [7].

The second design is a bent wire formed from three jointed orthogonal segments, having a total length of about one wavelength, as shown in Fig. 1(b). The transmission line has been replaced with a direct wire segment, maintaining a vertical distance of a quarter wavelength, but the electrical length is no longer a consideration. The two transverse straight wires, connected by the upright segment, are approximately three-eighths

Manuscript received October 11, 2005; revised March 30, 2006. This work was supported by the National Science Council under Grant 95-2752-E-009-003-PAE.

I-Y. Tarn is with the Department of Communication Engineering, National Chiao Tung University, Hsinchu, Taiwan, R.O.C. and also with the National Space Program Office (NSPO) of Taiwan, Hsin-Chu City, Taiwan, R.O.C. (e-mail: tarn.cm89g@nctu.edu.tw).

S.-J. Chung is with the Department of Communication Engineering, National Chiao Tung University, Hsinchu, Taiwan, R.O.C. (e-mail: sjchung@cm.nctu.edu.tw).

Digital Object Identifier 10.1109/TAP.2006.889802

wavelength and pointed in perpendicular directions. This structure can be fabricated in a laminate by using printed circuit technology: the two transverse wires are created by two metal traces and the vertical segment is accomplished by a conductive via.

For the CP wave illuminated at normal incidence that makes the respective induced currents on the two transverse wires in-phase, the two wires behave like dipoles with sinusoidal-like current distribution on them, and a null appears at the middle of the vertical segment. The entire bent wire thus operates at geometrical resonance, and the dipoles re-radiate waves in both the $+z$ and $-z$ directions. Below the substrate, the scattered wave propagates in the $-z$ direction, meanwhile above the substrate, the incident and scattered wave add 180° out of phase, thus producing a null field in that region.

For the other CP illumination, the induced currents on the two transverse wires are 180° out of phase, and tend to cancel each other out. The current distribution is much lower and no longer sinusoidal-like, and the scattered wave is thus much weaker. The reflected wave in this case is negligible and the incident wave in the transmission region is scarcely disturbed.

Although the second design is much simpler than the first one, implementing numerous, dense and thin vias on a CPSS accurately and stably is still hard to achieve in high frequencies. In printed circuit fabrication process, a vertical connection between layers is achieved by a via hole with copper plating on the walls and two annular ring pads encompassing the hole on each side of the substrate in order to avoid a peeling effect. The thickness of the copper plating for each via is usually inconsistent and will deteriorate the effectiveness of CP wave selectivity. Furthermore, poor conduction of the vias can lead to geometrical resonance phenomenon on the whole structures by undesired CP illumination, causing an increase in transmission loss.

To avoid the problems associated with the vertical conductive segments and increase flexibility in design motivated the drive to invent a new type of CPSSs that is composed of only transverse elements but no vias. Blocking electromagnetic waves at any designated frequency with two perpendicularly directed, adequately tuned dipoles which are placed a quarter wavelength apart is easy to do, but, if without the vias, both senses of CP wave will cause resonance on the two dipoles. In other words, the blocking effect works equally well for both RHCP and LHCP, and the inherency of CP wave selectivity is nonexistent.

In order to retain the capability of discriminating different CP waves, a substitute which is more suitable to multilayered printed circuit board (PCB) process is created in the midst of the two dipoles to take the place of the via. Connection would then be established through the couplings caused by the intermediate part between the two dipoles, so that each sense of circular polarization gives a different response. We construct the operational principle for this type of CPSSs, as described in Section II.

With the similarity of LHCPSS and RHCPSS, only the LHCPSS will be covered in this paper. Many simulations were performed using the commercial software HFSS [8]. From these simulations, the optimal parameters were obtained and a 30 GHz LHCPSS was designed and constructed. Lastly, the calculated and measured results are presented.

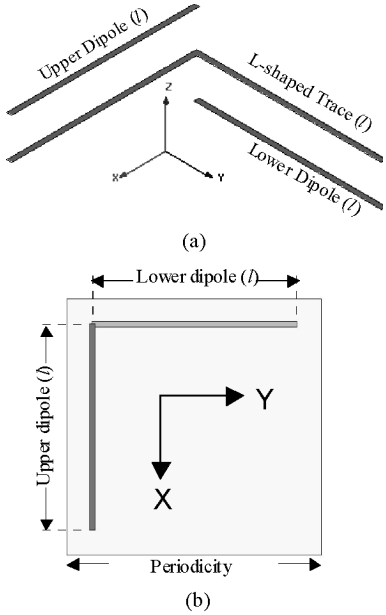

Fig. 2. (a) The unit cell of a CPSS that contains two perpendicular dipoles on top and bottom layers and an L-shaped trace in the middle. (b) Top view of the unit cell.

II. Principle

According to the fabrication capability provided by PCB manufacturers, both the minimum achievable trace width and spacing are 4 mils. In this paper, all trace widths and spacing are set to 0.1 mm (≈4 mils).

There are many commercially available, off-the-shelf products, which are suitable for the development of CPSSs. The selection of an appropriate laminate depends on the dielectric constant and the thickness of the substrate. A substrate with a dielectric constant of 2.33 and 62-mil thickness was chosen for our work, because it has the lowest error $(<5\%)$ at the designated frequency of 30 GHz.

For this paper, the term "Isolation" is defined as the amount of the designated polarization field blocked by the surface. The "isolation" for a LHCPSS is found by applying a LHCP plane wave illumination, then measuring the difference of the LHCP field intensity received with and without the LHCPSS inserted in front of the receiver. On the other hand, the "Transmission Loss" is found by measuring the difference of the RHCP field received with and without the LHCPSS inserted, with an input RHCP plane wave illumination.

The CPSSs presented in this paper, are arrays composed of identical cells made on dielectric slabs, with appropriate periodicities between cells. HFSS was employed to analyze the reflections and transmissions of the CPSSs. Perfectly matched layers (PMLs) were used to simulate an unbounded radiation environment. Periodic boundary conditions were applied to reduce the problem domain; consequently adopting only one unit cell for simulation is sufficient.

Fig. 2 illustrates a unit cell of a two-dimensional array, which contains two perpendicular dipoles located, respectively, on the top and bottom layers of a 62-mil Duroid 5870 laminate, with an L-shaped trace between the dipoles. The periodic boundary

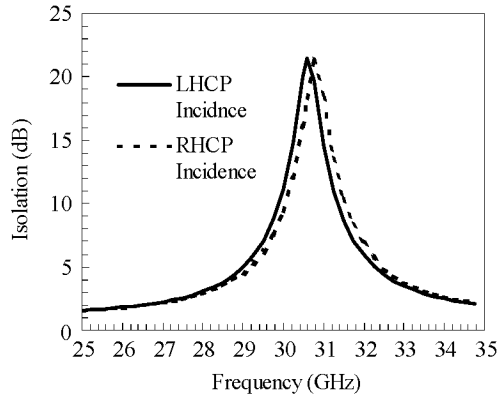

Fig. 3. Isolations as a function of frequency for a unit cell with two perpendicular dipoles located, respectively, on top and bottom layer of a 62-mil Duroid 5870 laminate ($l = 3.61$ mm, $\text{periodicity} = 4.5$ mm).

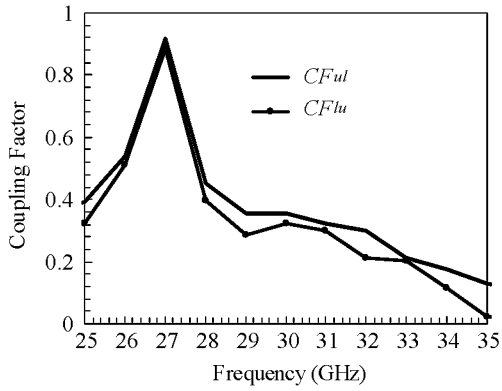

Fig. 4 Coupling factors as a function of frequency for the configuration shown in Fig. 2 ($l = 3.61$ mm, periodicity= 4.5 mm).

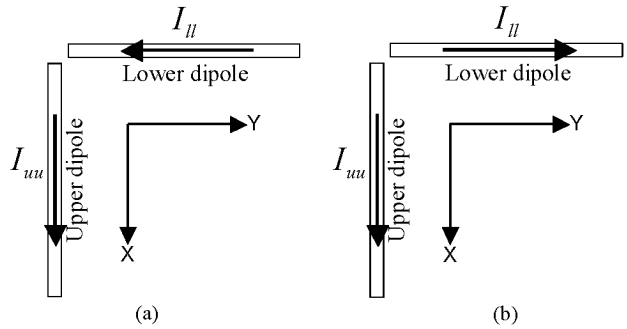

Fig. 5. The current directions on the upper and the lower dipoles excited by (a) LHCP incidence and (b) RHCP incidence, at 27 GHz.

conditions are applied on the four sidewalls of the cell, and the other two sides are attached with PMLs.

Consider if only the y-directed trace (lower dipole) existed in a unit cell (refer to Fig. 2), and illuminate the array with a normally incident $(+z)y$-polarized LP plane waves. The frequency response of isolation varies with the length of the dipole and the periodicity.

A maximum isolation of 20.76 dB at 30 GHz is found when $l = 3.61$ mm (about a half wavelength) with $\text{periodicity} = 4.5$ mm. The isolations for x-polarized incident plan wave are around 0.75 dB over the frequency range of 25–35 GHz, which can be regarded as the transmission losses in the substrate.

If the unit cell contains both upper and lower dipole, and the dipole lengths and periodicity remain the same, the simulated isolations as a function of frequency for respective LHCP and RHCP incidence are shown in Fig. 3. It confirms that a configuration with two perpendicularly directed dipoles separate one-quarter wavelength apart has almost the same blocking responses to LHCP and RHCP incidences. Also noted, was that the frequency the maximum isolation (21.5 dB) for a CP incidence occurred at, is a little higher than that for a LP incidence (30 GHz).

As stated in Section I, some coupling elements are needed to relate the upper and the lower dipole in such a way, that the whole structure exhibits CP wave selective property. An L-shaped trace was thus contrived as the coupling element, to be inserted into the middle of the two dipoles (Fig. 2). The dipole lengths and periodicity were kept unchanged. Each arm of the L-shaped trace has the same length as the dipoles and is parallel to the upper and the lower dipole, respectively.

With the addition of the L-shaped trace, the electromagnetic coupling effect generated causes the total effective currents on the upper and lower dipole to be primarily the vector sum of the currents as expressed in the following:

$$I_u = I_{uu} + I_{ul} = I_{uu} + \text{CF}_{ul} \cdot I_{ll} \quad (1)$$

$$I_l = I_{ll} + I_{lu} = I_{ll} + \text{CF}_{lu} \cdot I_{uu} \quad (2)$$

where I_u is the current on the upper dipole, I_l is the current on the lower dipole, I_{uu} is the current on the upper dipole induced by the x-component of the incident wave, I_{ll} is the current on the lower dipole induced by the y-component of the incident wave, I_{ul} is the current on the upper dipole coupled from the current on the lower dipole induced by the y-component of the incident wave, I_{lu} is the current on the lower dipole coupled from the current on the upper dipole induced by the x-component of the incident wave, and CF_{ul} and CF_{lu} are the coupling factors.

CF_{ul} is defined as the ratio of the magnitudes, of the currents on the upper dipole, with respect to the magnitudes of the currents on the lower dipole, when excited by a y-polarized plane wave; whereas CF_{lu} is the ratio of the magnitudes, of the currents on the lower dipole, with respect to the magnitudes of the currents on the upper dipole, when excited by an x-polarized plane wave. The simulated coupling factors for various frequencies are shown in Fig. 4. It was discovered that CF_{ul} is very close to CF_{lu}, and the maximum coupling factor of about 0.92 occurs at 27 GHz. The directions of the current for the upper and the lower dipoles excited by LHCP and RHCP incidences at this frequency are indicated in Fig. 5, and the directions of the current on the upper and the lower dipoles excited by x- and y-polarized plane waves, respectively, are indicated in Fig. 6.

For a 27 GHz LHCP illumination, I_{ll} and I_{lu} are in the same direction, and I_{uu} and I_{ul} are also in the same direction. Therefore, by (1) and (2), the currents on both dipoles add constructively. The geometrical resonance remains on the dipoles, so that a LHCP wave is reflected.

On the contrary, for a 27 GHz RHCP illumination, I_{lu} and I_{ll} are approximative in magnitude but opposite in direction, as are I_{ul} and I_{uu}. The mutual interactions make the currents on the

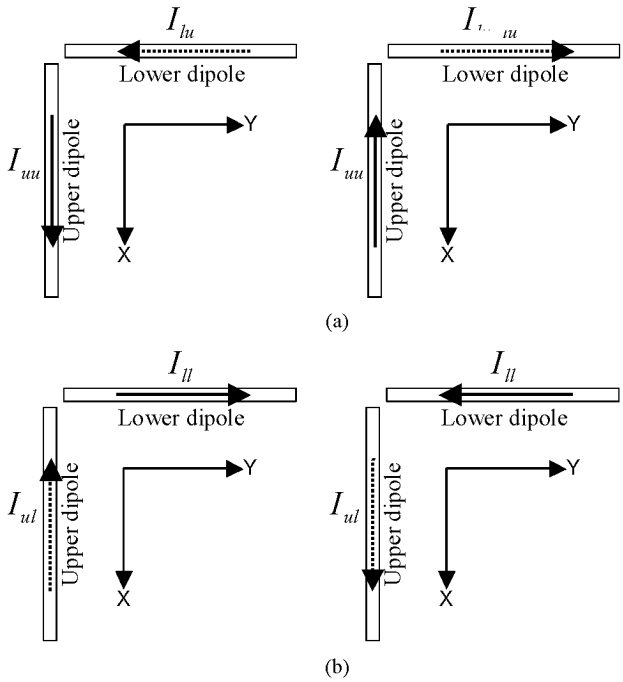

Fig. 6. The current directions on the upper and the lower dipoles excited by (a) 27 GHz x-polarized plane waves and (b) 27 GHz y-polarized plane waves. The dashed line indicates the coupled currents.

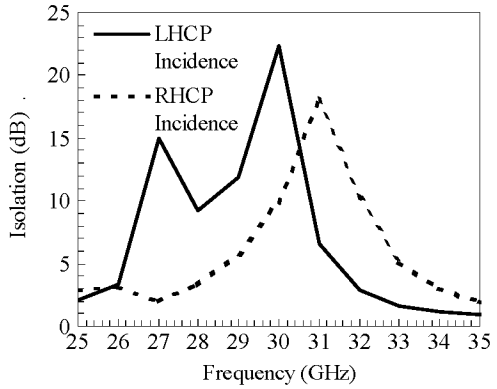

Fig. 7. The simulated isolations as a function of frequency for the configuration shown in Fig. 2 ($l = 3.61$ mm, $\mathrm{periodicity} = 4.5$ mm).

dipoles nearly cancelled out, allowing the incident RHCP wave to pass through this type of CPSSs with only a slight influence as a result of the much-reduced scattered fields ascribed to the L-shaped trace.

The simulated isolations as a function of frequency for LHCP and RHCP incidences are shown in Fig. 7. The results reveal that the isolation curves for LHCP and RHCP are no longer similar, as compared with Fig. 3. At 27 GHz, a sudden rise in LHCP isolation curve can be seen, but the isolation slightly declines for RHCP incidence, as expected. Consequently, it is reasonable to conclude that the coupling effect generated by the presence of the L-shaped trace in between the upper and lower dipole markedly affects the circular polarization selectivity performance of a CPSS structure.

Further investigations on the L-shaped trace were performed to better understand its property. Simulated results show that

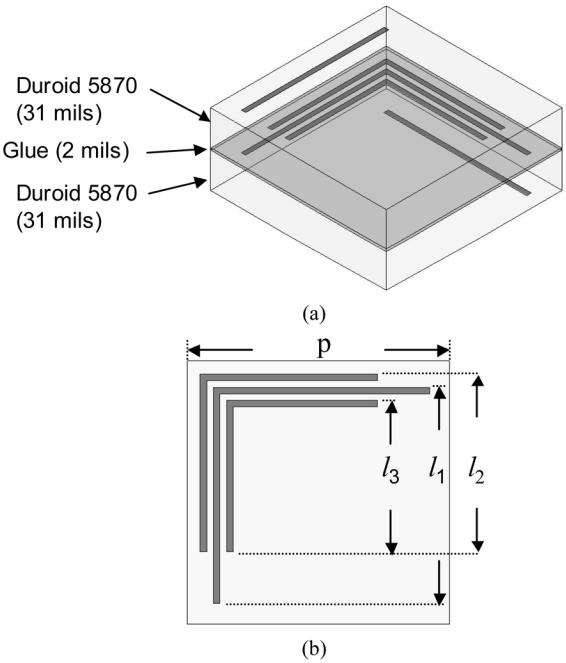

Fig. 8. (a) The schema of the proposed LHCPSS configuration. (b) Top view of a unit cell of the LHCPSS, three L-shaped traces are implemented in the middle layer.

when the length of the L-shaped trace gets longer, the maximum coupling factor shifts towards lower frequency. Therefore, the lengths of the arms of the L-shaped trace should be slightly shorter than the lengths of the dipoles in order to have a higher isolation for LHCP incidence and a lower transmission loss for RHCP incidence at the desired frequency.

III. Design

With the function of the L-shaped trace confirmed, we added two auxiliary L-shaped traces in order to enhance the coupling effect and increase degrees of freedom in designing. The additional L-shaped traces are also in the middle layer but placed on either side of the original L-shaped trace. The lengths of the two additional traces are variables, independent of the length of the central L-shaped trace. Being a three-layered structure, two 31-mil Duroid 5870 laminates are utilized to develop the LHCPSS, and the L-shaped traces are implemented on the bottom side of the upper laminate. A coat of agglutinate substance binds the laminates together, with a minimum achievable thickness of the agglutinate substance being 2 mils. Initially, the agglutinate substance is assumed to be made of the same material as the substrates (Duroid 5870) above and below. The whole configuration is illustrated in Fig. 8(a).

Preliminary simulations show that the two additional L-shaped traces, in contrast to the original one, have minor contribution in reducing the RHCP induced currents on the upper and the lower dipoles. Furthermore, no significant improvements were obtained by having unmatched endpoints, or end-edges of the two additional L-shaped traces which are not in same straight lines. Therefore, to decrease the calculation amount, all simulations will be performed with the two additional L-shaped traces having matching endpoints.

The geometry variables used for optimization are indicated in Fig. 8(b).

The performance of the circular polarization selectivity is extremely sensitive to the lengths of the traces; especially the lengths of the two dipoles. The lengths of the dipoles on the top and bottom layers primarily determine the LHCP isolation of a LHCPSS, while the well-tuned L-shaped traces in the middle layer would reduce the RHCP transmission loss. The periodicity of the array has an analogous effects on both the isolation and transmission loss; the larger the periodicity, the less the isolation and transmission loss.

The optimization process starts by first assuming that the lengths of the two dipoles are a half wavelength in the substrate, without any other metallic traces. With this design, excellent isolations (e.g., beyond 40 dB by simulation) can be achieved by varying the dipole lengths, however, high transmission losses accompanies. Next, the three L-shaped traces are taken into account, and lastly the periodicity of the array is included. With the combination of these, we have a total of four degrees of freedom available for optimization; they are the lengths of the metallic traces (l, l_1, and l_3) as well as the periodicity of the array (p), provided that $l_2 = l_3 + 0.4$ mm (see Fig. 8). All of the geometry variables affect the result, so for the optimum solution, all four variables must be adjusted simultaneously.

Then, find the geometry which gives good isolation and acceptable transmission loss. The geometry parameters obtained are: $p = 4$ mm, $l = 3.25$ mm, $l_1 = 3.295$ mm, $l_2 = 2.7$ mm, and $l_3 = 2.3$ mm. The resultant isolation is 19.83 dB and the transmission loss is about -2.55 dB. Note that l_1 is a little longer than l, which violates the inferences we drew in Section II. The geometry does not have to be the perfect, because the glue is not made of Duroid 5870 material in reality, it is merely treated as an initial step to be followed up with optimizations.

For the purpose of examining the effects of the glue, simulations were done with the geometry unchanged, but replacing the glue layer with different materials. As Figs. 9 and 10 indicate, the isolation is a rapidly varying function of ε_r, while the transmission loss is a slowly varying one. $\varepsilon_r = 2.33$ is the special case where the agglutinate substance is of the same material as the substrates. The performance of the design is considerably susceptible to the agglutinate substance. Therefore the geometry should be redesigned to overcome the influence brought about by the glue.

Also of interests, is to vary the glue thicknesses to investigate its interaction, because the glue thickness is hard to control. In Figs. 9 and 10, isolations and transmission losses for different glue thicknesses shows little change. This signifies that the height of the configuration is less important as a factor; the spacing between the upper and the lower dipole do not affect the performance much with this design.

FR-4 ($\varepsilon_r = 4.5$) is the most commonly used agglutinate substance by manufacturers to glue printed circuit boards together. Under this condition, achieving optimal geometries are not convenient because the agglutinate substance is different from the substrates of the laminates. The discontinuities caused by different materials lead to additional reflections. Fig. 9 shows the isolations for the initial design with $\varepsilon_r = 4.5$ glue, fall to less than 5 dB.

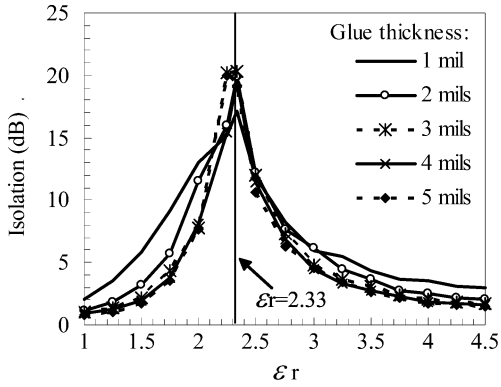

Fig. 9. Isolations at 30 GHz for various ε_r and thicknesses of the glue layer ($p = 4$ mm, $l = 3.25$ mm, $l_1 = 3.295$ mm, $l_2 = 2.7$ mm, and $l_3 = 2.3$ mm).

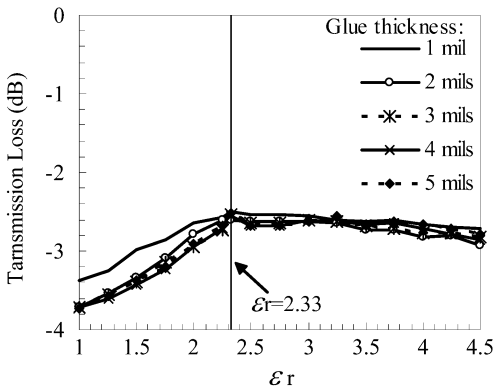

Fig. 10. Transmission losses at 30 GHz for various ε_r and thicknesses of the glue layer ($p = 4$ mm, $l = 3.25$ mm, $l_1 = 3.295$ mm, $l_2 = 2.7$ mm, and $l_3 = 2.3$ mm).

If there is no metal trace or dipole, i.e., only substrates and glue layer exist, the transmission losses for the same ranges of ε_r and glue thicknesses as in Fig. 10 are between -0.64 dB and -0.95 dB. The transmission loss for a 2-mil FR-4 glue layer is about -0.86 dB, which can be explained as the loss caused by the substrates and glue layer.

The optimization procedure described above is resumed to find the proper geometry parameters of the present configuration with a 2-mil FR-4 glue layer. By iteratively adjusting l_1 and l_3 together with p for various dipole lengths (l), and then sifting out the cases with high isolation and low transmission loss, the appropriate solutions can be extracted. Some of the selected results are shown in Fig. 11.

Tradeoffs will have to be made, to give consideration to both, low transmission loss and high isolation. The criterion used to judge the optimized geometry is for a case that has the highest isolation with a transmission loss of no worse than -2.5 dB. The final parameters are determined as follows: $p = 6.25$ mm, $l = 3.385$ mm, $l_1 = 2.9$ mm, $l_2 = 3.0$ mm, and $l_3 = 2.6$ mm. Consequently, LHCP isolation and RHCP transmission loss for the proposed structure at 30 GHz are 12.52 dB and -2.36 dB, respectively.

Fig. 12 illustrates the normalized induced current distributions, on the optimized LHCPSS for LHCP and RHCP emanations, respectively. As can be seen, the current for the LHCP wave is much higher and appears as a resonant distribution,

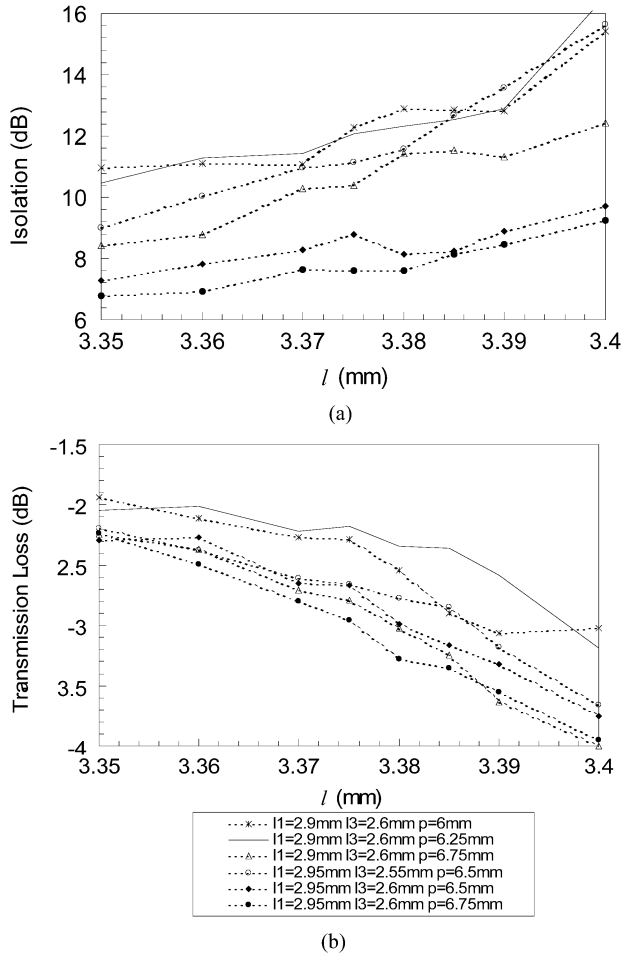

Fig. 11. (a) Simulated isolations for several geometrical variables (l_1, l_3, p) with respect to l. (b) Simulated transmission losses for several geometrical variables (l_1, l_3, p) with respect to l.

while the RHCP wave exhibits much less current and very little resonance.

IV. Measurement

Fig. 13 is the finished LHCPSS with 185 unit elements, made on a disk-shape substrate, with a radius of about 55 mm.

Measurements are performed with an Agilent 8510C vector network analyzer. Due to the lack of standard CP horn antenna, two standard LP horn antennas are installed on the two ends of the network analyzer. The cross-polarization levels of the LP horns are less than -40 dB, whose effects are neglected in the following analysis. These two horns are collimated and aligned with each other, as sketched in Fig. 14. For shielding, a metal plate with a hole having the same radius as the CPSS is placed in between the two horns. The LHCPSS under test is installed in place of the hole. Phase compensation was not taken into consideration in designing, so the distances between the LHCPSS and the two horns must be large enough to ensure the phase of the wave to be uniformly distributed over the aperture of the LHCPSS. In our setup, the distances are set to 60 cm. Fig. 15 is the picture taken during measurements.

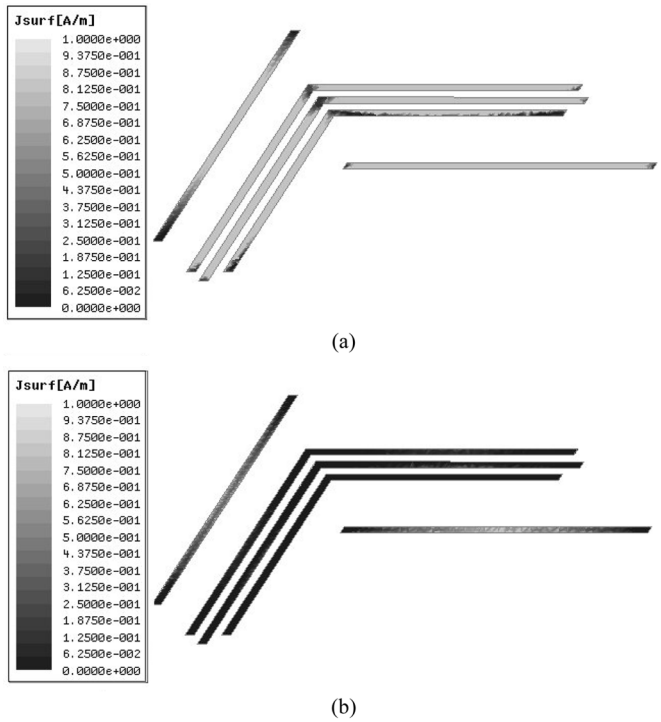

Fig. 12. Normalized induced current on the metallic traces of the optimized LHCPSS illuminated with (a) LHCP wave and (b) RHCP wave.

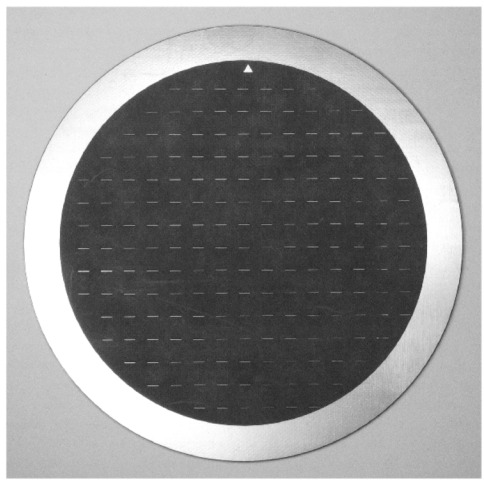

Fig. 13. Photograph of the finished LHCPSS, with 185 elements on a disk-shape substrate. The radius of the disk is about 55 mm.

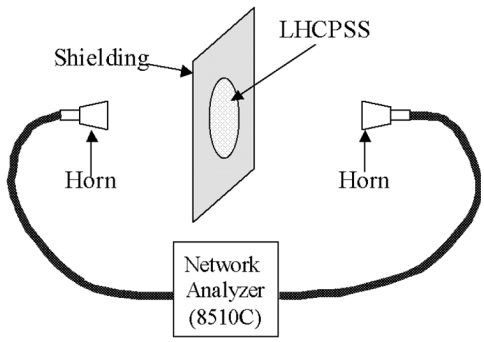

Fig. 14. Schematic of the measurement setup.

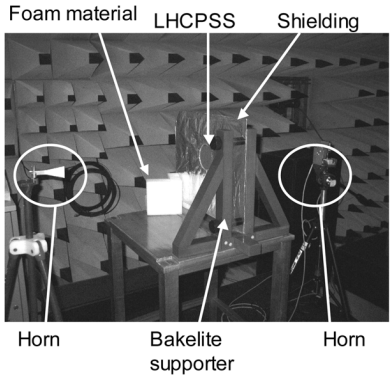

Fig. 15. Picture taken during measurements. Two LP horn antennas are placed about 60 cm apart, and the LHCPSS under test is put in the midst of them.

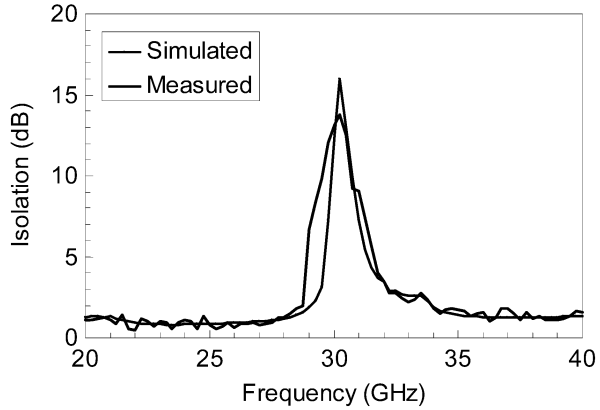

Fig. 16. The simulated and measured isolations for the LHCPSS of $p = 6.25$ mm, $l = 3.385$ mm, $l_1 = 2.9$ mm, $l_2 = 3.0$ mm, and $l_3 = 2.6$ mm.

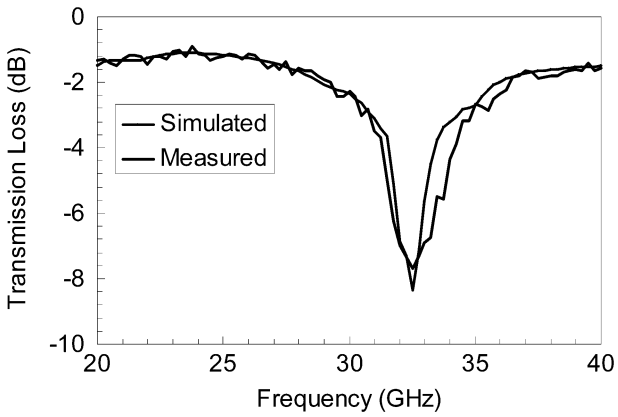

Fig. 17. The simulated and measured transmission losses for the LHCPSS of $p = 6.25$ mm, $l = 3.385$ mm, $l_1 = 2.9$ mm, $l_2 = 3.0$ mm, and $l_3 = 2.6$ mm.

Let E_{Major} and E_{Minor} be the electric field magnitudes in respective major and minor axis of the polarization ellipse of a CP wave

$$E_{\text{Major}} = \frac{E_{R0} + E_{L0}}{2} \tag{3}$$

$$E_{\text{Minor}} = \frac{E_{R0} - E_{L0}}{2} \tag{4}$$

where E_{L0} and E_{R0} denote the intensities of left- and right-hand components, respectively.

By definition, the axial ratio (AR) of a CP wave is

$$|\text{AR}| = \frac{E_{\text{Major}}}{E_{\text{Minor}}} = \frac{E_{R0} + E_{L0}}{E_{R0} - E_{L0}} = \frac{1 + (E_{L0}/E_{R0})}{1 - (E_{L0}/E_{R0})}. \tag{5}$$

Rotate the receiving horn and the LHCPSS under test until maximum and minimum S_{21} appear, the axial ratio can be calculated from (5) and E_{L0}/E_{R0} can be derived from

$$\frac{E_{L0}}{E_{R0}} = \frac{|\text{AR}| - 1}{|\text{AR}| + 1}. \tag{6}$$

Suppose that the transmission loss of the RHCP component compared to the reduction in the LHCP component, caused by the LHCPSS, is negligible, i.e., $E_{R0} > E_{L0}$ at the receiving side, E_{L0} and E_{R0} can be deduced from the measured maximum and minimum S_{21}.

Remove the LHCPSS, while keeping the shielding plate in place, re-perform the S_{21} measurement to figure out the referenced LHCP and RHCP components of the incident wave, and then follow the definitions described in Section II, the isolation and transmission loss can be obtained.

Fig. 16 shows the frequency response of the measured isolation for the realized LHCPSS. The simulated response is also shown for comparison. The figure indicates that the measured data is very similar to the simulated one. The maximum measured isolation of 13.78 dB was obtained at 30.2 GHz, and the maximum simulated isolation of about 16 dB occurred at 30.25 GHz. The isolation measured at 30 GHz is 13.12 dB, while the simulated one is 12.52 dB.

Fig. 17 illustrates the corresponding transmission losses for the measurements and simulations. The transmission loss of the realized LHCPSS also closely resembles that of the simulated one. Transmission loss of about -2.28 dB was measured at 30 GHz, while the simulated one is -2.36 dB. It is reminded that the loss caused by the substrates and glue layer of about -0.86 dB has been included in the transmission loss, as was mentioned in Section III.

The designing of a LHCPSS with better transmission loss would be possible at the target frequency of 30 GHz, but it would have come at the expense of a better isolation.

Comparing Fig. 9 with Fig. 16, it is obvious that the isolation at 30 GHz for 2-mil FR-4 glue has been enhanced, although less when compared to the isolation with Duroid 5870 as the agglutinate substance. In summary, it clearly demonstrates that improvements with the degradation in isolation caused by the material and thickness of the agglutinate substance can be overcome with optimization in this design.

V. Conclusion

In this paper, a LHCPSS with simple concept is simulated and fabricated. The measured data of the finished LHCPSS and the simulated results show good consistency, having isolation of larger than 13 dB for an incident LHCP wave at 30 GHz, with transmission loss of -2.28 dB for the RHCP wave.

The LHCPSS presented is a thoroughly stratified configuration with transverse planar elements implemented on different

layers. The L-shaped traces accomplish the function that formerly had to be performed by vertical conductive segments. Avoiding the uses of vertical conductive segments makes this design well suited for PCB manufacturing process. By dint of the L-shaped traces, the frequency responses of blocking effect for different CP illuminations are diverse. At 30 GHz, LHCP incidence is blocked because of strong geometry resonance on dipoles, whereas RHCP incidence passes because of little or weak geometry resonance. Thus the CPSS is selective to the sense of CP waves.

More noteworthy, is that this new concept provides more flexibility in developing CPSSs. This CPSS design is more tolerable to the thickness and the material of the substrate. The height of the whole configuration is no longer strictly required to be a quarter wavelength, because the connection between each pair of dipoles in a unit cell, no longer relies on the vertical conductive segment, but the couplings caused by the L-shaped traces between dipoles. Laminates with various substrates and different thicknesses rather than one-quarter wavelength can be used to realize a CPSS with satisfactory performance by the method presented in this paper. The completion of this work demonstrates the feasibility of this new type of CPSSs. Structures with superior performance may be created from the basis of this paper.

Successful development of such surfaces will have several applications. For example, a good CPSS can be used as the sub-reflector of a Cassegrain antenna. The manufacturing of a planar CPSS is much easier than a curved sub-reflector. In addition, this type of Cassegrain antenna will have a minimal aperture blockage, because the CP waves reflected by the main reflector would pass through the CPSS almost without loss.

As a second example, the linear polarizer in the original LP folded reflectarray antenna would be replaced by a CPSS. The main reflector design would no longer be applicable, as it would be a simple flat conducting plate in this CP version. With the emergency of excellent CPSSs, folded reflectarray could be extended to circular polarization applications.

REFERENCES

[1] D. G. Berry, R. G. Malech, and W. A. Kennedy, "The reflectarray antenna," *IEEE Trans. Antennas Propag.*, vol. 11, pp. 645–651, Nov. 1963.

[2] D. Pilz and W. Menzel, "Folded reflectarray antenna," *Electron. Lett.*, vol. 34, pp. 832–833, Apr. 1998.

[3] J. Huang and R. J. Pogorzelski, "Microstrip reflectarray with elements having variable rotation angles," in *IEEE AP-S Int. Symp. Digest*, Jul. 1997, vol. 2, pp. 1280–1283.

[4] C.-P. Chiu and S.-J. Chung, "A new millimeter-wave folded microstrip reflectarray antenna with beam steering," in *IEEE AP-S Int. Symp. Digest*, Jun. 2002, vol. 3, pp. 140–143.

[5] D. Pilz and W. Menzel, "A novel linear-circular polarization converter," in *Proc. 28th Europ. Microw. Conf.*, Amsterdam, 1998, pp. 18–23.

[6] W. V. Tilson, T. Tralman, and S. M. Khanna, "A polarization selective surface for circular polarization," in *IEEE AP-S Int. Symp. Digest*, Jun. 1988, vol. 2, pp. 762–765.

[7] G. A. Morin, "A simple circular polarization selective surface," in *IEEE AP-S Int. Symp. Digest*, May 1990, vol. 1, pp. 100–103.

[8] [Online]. Available: http://www.ansoft.com/products/hf/hfss/

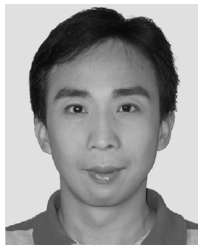

I-Young Tarn was born in Taipei, Taiwan, R.O.C. He received the B.S. and M.S. degrees in electrical engineering from Yuan-Ze University, Tao-Yuan, Taiwan, R.O.C., in 1993 and 1995, respectively, and is currently working toward the Ph.D. degree in communication engineering at the National Chiao Tung University, Hsinchu, Taiwan, R.O.C.

From 1995 to 1999, he was an Assistant Researcher in Systems Engineering Project, National Space Program Office, Hsinchu, Taiwan, R.O.C. Since 2000, he has been with the Electrical Engineering Division of the National Space Program Office, where he has been involved in satellite communications and antenna design. His research interests include microwave/mm-wave planar antennas, reflectarray antennas, circular polarization selective structures and satellite antenna design and verification.

Shyh-Jong Chung (M'92–SM'06) was born in Taipei, Taiwan, R.O.C. He received the B.S.E.E. and Ph.D. degrees from National Taiwan University, Taipei, Taiwan, R.O.C., in 1984 and 1988, respectively.

Since 1988, he has been with the Department of Communication Engineering, National Chiao Tung University, Hsinchu, Taiwan, R.O.C., where he is currently a Professor. From September 1995 to August 1996, he was a Visiting Scholar with the Department of Electrical Engineering, Texas, A&M University, College Station. He has authored or coauthored over 70 technical papers in international journals or conferences including several invited papers and speeches. His areas of interest include the design and applications of active and passive planar antennas, communications in intelligent transportation systems (ITSs), LTCC-based RF components and modules, packaging effects of microwave circuits, and numerical techniques in electromagnetics.

Dr. Chung serves as the Chairman of IEEE MTT-S Taipei Chapter from 2005. He was also the Treasurer of IEEE Taipei Section from 2001 to 2003.